ZANCO Journal of Pure and Applied Sciences
The official scientific journal of Salahaddin University-Erbil
https://zancojournals.su.edu.krd/index.php/JPAS

ISSN (print):2218-0230**, ISSN (online):** 2412-3986**, DOI: http://dx.doi.org/10.21271/zjpas**

RESEARCH PAPER

Hopf Bifurcation and Global Dynamics Analysis of Generalized Sprott L System

Azad I. Amen[1,2,3,4], Hassan A. Ahmad[2]
1 Department of Mathematics, College of Basic Education, Salahaddin University -Erbil, Iraq.
2 Department of Mathematics, Basic Education College, Raparin University-Ranya, Iraq
3 Department of Mathematics, Faculty of Science, Soran University, Soran, Erbil, Iraq.
4 Department of Mathematics, College of Science, Duhok University, Iraq.

A B S T R A C T:
A simple chaotic L system with only one nonlinearity and five terms was introduced by Sprott. We consider the generalized Sprott L differential system $\dot{x} = y + \alpha z, \dot{y} = \beta x^2 - y, \dot{z} = \delta - x,$ where $\beta \neq 0, \alpha$ and δ represent real parameters. We study the local stability of equilibrium points, in particular, by choosing an appropriate bifurcation parameter, the paper proves that Hopf bifurcation occurs in the system, and presents a formula for determining the direction of the Hopf bifurcation and the stability of bifurcating periodic solutions by applying normal form theory. Moreover, we study the dynamics near and at infinity by using the Poincar´e compactification to describe the global dynamics of the trajectories of the system. Our results show that the real parameters do not affect the global dynamics at infinity of the system.

KEY WORDS: Generalized Sprott L system; Hopf bifurcation; Poincare compactification; Dynamics at infinity. .
DOI: http://dx.doi.org/10.21271/ZJPAS.35.SpB.5
ZJPAS (2023) , 35(SpB);42-50 .

1. INTRODUCTION

In the past few decades, extensive research has been done on chaos, an intriguing occurrence in nonlinear dynamical systems. A nonlinear deterministic system that exhibits complicated and unpredictable behavior is called a chaotic system. Chaos theory has many applications in a variety of ways in the natural sciences (Guckenheimer & Holmes, 2013; Sprott, 1994). Bifurcation is the most important theory for the qualitative investigation of dynamical systems and can be used to reveal complex dynamical characteristics of the system under consideration. Characterizing the existence of periodic solutions is one of the more basic issues in the qualitative theory of differential systems in three dimensions. A family of periodic solutions can bifurcate from a known family of equilibrium points in a dynamical system using the Hopf bifurcation, which provides the simplest criterion (Jiang, Han & Qinsheng, 2010).

Suppose that the nonlinear autonomous system

$$\dot{X} = f(X;\mu)\ , X \in R^3, \mu \in R,$$

has an isolated equilibrium point $X(\mu)$, where μ is bifurcation parameter at which the following conditions are satisfied.

1. The Jacobian matrix $D_x f(\mathrm{X}(\mu)), \mu)$ has a pair of complex eigenvalues $\lambda_{1,2} = a(\mu) \pm i\omega(\mu)$ and another eigenvalue $\lambda_3 < 0$ with $\omega(\mu_0) = \omega_0 > 0, a(\mu_0) = 0.$
2. $\frac{d}{d\mu}(Re(\lambda(\mu_0)) \neq 0$, where λ be any eigenvalue of Jacobian matrix.

Then, there exists a family of periodic solutions bifurcating at (X, μ_0), for more details see (Amen & Salih 2008; Jiang, Han & Qinsheng, 2010; Mirkhan & Amen, 2022; Moiola & Chen, 1996).

* **Corresponding Author:**
Azad I. Amen
E-mail: azad.amen@su.edu.krd
Article History:
Received: 10/07/2023
Accepted: 17/08 /2023
Published: 01/ 11/2023

The polynomial differential system (1) listed below, like any polynomial vector field, can be extended to an analytic system on a closed ball of radius one, whose interior is diffeomorphic to $\mathbb{R}^3$ and whose boundary, sphere $\mathbb{S}^2$ is invariant by the flow of the extended system and plays the role to infinity. The method for creating such an extension is the well-known Poincar´e compactification for polynomial vector fields, which is described in (Cima & Llibre, 1990). The sphere $\mathbb{S}^2$, which represents the points at infinity in this context, is referred to as Poincar´e sphere. Also, in (Messias, 2011), a summery about Poincar´e compactification for a polynomial vector field in $\mathbb{R}^3$ is provided for understanding section 3 of this paper.

Sprott suggested 19 straightforward chaotic flows known as Sprott A-S systems in 1994 (Sprott, 1994), where the generalized Sprott L system is described by the following first order autonomous differential equations

$$\dot{x} = y + \alpha z,\ \dot{y} = \beta x^2 - y,\ \dot{z} = \delta - x, \quad (1)$$

depending on three real parameters α, δ and $\beta \neq 0$. As usual, the dot denotes the derivative with respect to the time t. This system for $\alpha = 3.9, \beta = 0.9$ and $\delta = 1$ is the Sprott L system and exhibits a strange chaotic attractor (Sprott, 1994). The characteristics of system (1), including their critical points, Lyapunov exponents and fractal dimensions, are studied in (Sprott, 1994). Results for the Sprott L system's global chaotic synchronization utilizing the active control method were derived in the article (Vaidyanathan, 2012).

In this study, we have two main goals. The first goal is to analyze the existence of a Hopf bifurcation in System (1), by selecting a suitable bifurcation parameter and applying the normal form theory. This will lead to the birth of a limit cycle (isolated closed orbits) from an equilibrium point of the system.

The second one is to study dynamical behavior at infinity. In order to fully describe the dynamics of system (1) on the sphere $\mathbb{S}^2$ at infinity, we employ the Poincar´e compactification described above. This will help us understand how the solutions, depending on the parameter values, approach and depart from infinity.

2. Local Stability of Equilibrium Points and Hopf Bifurcation Analysis

We now compute the equilibrium points of system (1). By simple analysis, it is easy to obtain that if $\alpha \neq 0$ system (1) has only one equilibrium point $\mathrm{E}_1(\delta, \beta\delta^2, -\frac{\beta\delta^2}{\alpha})$. While when $\alpha = 0$ and $\delta = 0$, system (1) has a non-isolated equilibrium points $\mathrm{E}_2(0,0,z)$, for all real number z . But if $\alpha = 0$ and $\delta \neq 0$, then system (1) has no equilibrium points.

Proposition 1. For system (1).
1. If $\alpha > 0$ and $\beta\delta < 0$, then the equilibrium point E_1 is asymptotically stable.
2. If $\delta = 0$ and $\alpha < 0$, then the equilibrium point E_1 is unstable.

Proof. 1. The characteristic equation of the Jacobian matrix at the equilibrium point E_1 of system (1) is given by

$$\lambda^3 + \lambda^2 + (-2\beta\delta + \alpha)\lambda + \alpha = 0. \quad (2)$$

When $\alpha > 0$ and $\beta\delta < 0$, so by the Routh-Hurwitz criterion, the zeros of the above characteristic equation have negative real parts. Hence, the equilibrium point E_1 is asymptotically stable.
2. When $\delta = 0$, equation (2) becomes

$$\lambda^3 + \lambda^2 + \alpha\lambda + \alpha = 0. \quad (3)$$

if $\alpha < 0$, then equation (3) has exactly one positive root by using Descartes' rule of signs, then the equilibrium point E_1 is unstable. ■

Proposition 2. (Occurrence of Hopf bifurcation**)**
The characteristic equation (2) has a pair of purely imaginary conjugate eigenvalues $\lambda_{1,2} = \pm i\omega = \pm i\sqrt{\alpha}$ with a real eigenvalue $\lambda_3 = -1$ if and only if $\delta = 0$ and $\alpha > 0$, then system (1) undergoes the Hopf bifurcation at the equilibrium point E_1, provide that $\beta \neq 0$.

Proof. It is very simple to show that the characteristic equation (2) has a pair of purely imaginary conjugate eigenvalues with a negative eigenvalue if and only if $\delta = 0$ and $\alpha > 0$. Then if $\delta = 0$ we get the characteristic equation (3) as given below

$$\lambda^3 + \lambda^2 + \alpha\lambda + \alpha = 0.$$

Transform to

$$(\lambda+1)(\lambda^2+\alpha)=0. \quad (4)$$

Hence, equation (4) has a pair purely imaginary conjugate eigenvalues $\lambda_{1,2}=\pm i\sqrt{\alpha}$,$\alpha>0$ with a real eigenvalue $\lambda_3=-1$. We can choose δ is a bifurcation parameter and the critical value is $\delta=\delta_0=0$. Using the implicitly differentiating $\lambda=\lambda(\delta_0)$ in equation (2) we get

$$\frac{d\lambda}{d\delta}=\frac{2\beta\lambda}{3\lambda^2+2\lambda+\alpha}.$$

Hence, we obtain

$$Re\left(\frac{d\lambda}{d\delta}\right)_{\delta=\delta_0,\lambda=i\sqrt{\alpha}}=\frac{\beta}{\alpha+1}\neq 0,$$

and

$$Im\left(\frac{d\lambda}{d\delta}\right)_{\delta=\delta_0,\lambda=i\sqrt{\alpha}}=-\frac{\beta\sqrt{\alpha}}{\alpha+1}\neq 0.$$

Therefore, the first and second conditions of Hopf bifurcation are satisfied. However, in order to use the Hopf bifurcation Theorem (Guckenheimer & Holmes, 2013). Then system (1) undergoes the Hopf bifurcation at the equilibrium point E_1. ■

Now, we investigate the direction, stability and period of the bifurcating periodic solution for system (1) at the equilibrium point E_1, by applying normal form theory (Hassard & Wan, 1978).

First, we make the change of variables

$$(x,y,z)=(x_1+\delta,y_1+\beta\delta^2,z_1-\frac{\beta\delta^2}{\alpha}),$$

which means, we move the equilibrium point $(\delta,\beta\delta^2,-\frac{\beta\delta^2}{\alpha})$ to the origin, then system (1) becomes

$$\begin{aligned}\dot{x_1}&=y_1+\alpha z_1,\\ \dot{y_1}&=\beta x_1^2+2\beta\delta x_1-y_1,\\ \dot{z_1}&=-x_1.\end{aligned} \quad (5)$$

Now, we find that the eigenvectors correspond to the eigenvalues λ_1 and λ_3, suppose that v_1+iv_2 is an eigenvector correspond $\lambda_1=i\sqrt{\alpha}$ and v_3 is an eigenvector correspond $\lambda_3=-1$ as given below

$$v_1=\begin{pmatrix}0\\0\\1\end{pmatrix},\quad v_2=\begin{pmatrix}-\sqrt{\alpha}\\0\\0\end{pmatrix},\quad v_3=\begin{pmatrix}1\\-1-\alpha\\1\end{pmatrix}.$$

Let

$$T=(v_2\quad v_1\quad v_3)=\begin{pmatrix}-\sqrt{\alpha}&0&1\\0&0&-1-\alpha\\0&1&1\end{pmatrix}.$$

We take the following change $\begin{pmatrix}x_1\\y_1\\z_1\end{pmatrix}=T\begin{pmatrix}x_2\\y_2\\z_2\end{pmatrix}$, for system (5) so we get

$$\begin{aligned}\dot{x_2}&=-\sqrt{\alpha}y_2+P_1(x_2,y_2,z_2),\\ \dot{y_2}&=\sqrt{\alpha}x_2+Q_1(x_2,y_2,z_2),\\ \dot{z_2}&=-z_2+R_1(x_2,y_2,z_2),\end{aligned} \quad (6)$$

where

$$\begin{aligned}P_1(x_2,y_2,z_2)&=-\frac{\beta\sqrt{\alpha}\,x_2^2}{1+\alpha}+\frac{2\beta x_2z_2}{1+\alpha}-\frac{\beta z_2^2}{\sqrt{\alpha}(1+\alpha)},\\ Q_1(x_2,y_2,z_2),&=\frac{\beta\alpha\,x_2^2}{1+\alpha}-\frac{2\beta\sqrt{\alpha}x_2z_2}{1+\alpha}+\frac{\beta z_2^2}{(1+\alpha)},\\ R_1(x_2,y_2,z_2)&=-\frac{\beta\alpha\,x_2^2}{1+\alpha}+\frac{2\beta\sqrt{\alpha}x_2z_2}{1+\alpha}-\frac{\beta z_2^2}{(1+\alpha)}.\end{aligned} \quad (7)$$

By using proposed by Hassard *et al* and described in (Hassard & Wan, 1978), we work to calculated the following quantities and all quantities are calculated at $\alpha>0$ and $(x_2,y_2,z_2)=(0,0,0)$.

$$g_{11}=\frac{1}{4}\left(\frac{\partial^2P_1}{\partial x_2^2}+\frac{\partial^2P_1}{\partial y_2^2}+i\left(\frac{\partial^2Q_1}{\partial x_2^2}+\frac{\partial^2Q_1}{\partial y_2^2}\right)\right)=-\frac{\beta\sqrt{\alpha}}{2(1+\alpha)}+\frac{i\beta\alpha}{2(1+\alpha)},$$

$$g_{02}=\frac{1}{4}\left(\frac{\partial^2P_1}{\partial x_2^2}-\frac{\partial^2P_1}{\partial y_2^2}-2\frac{\partial^2Q_1}{\partial x_2\partial y_2}+i\left(\frac{\partial^2Q_1}{\partial x_2^2}-\frac{\partial^2Q_1}{\partial y_2^2}+2\frac{\partial^2P_1}{\partial x_2\partial y_2}\right)\right)=-\frac{\beta\sqrt{\alpha}}{2(1+\alpha)}+\frac{i\beta\alpha}{2(1+\alpha)},$$

$$g_{20}=\frac{1}{4}\left(\frac{\partial^2P_1}{\partial x_2^2}-\frac{\partial^2P_1}{\partial y_2^2}+2\frac{\partial^2Q_1}{\partial x_2\partial y_2}+i\left(\frac{\partial^2Q_1}{\partial x_2^2}-\frac{\partial^2Q_1}{\partial y_2^2}-2\frac{\partial^2P_1}{\partial x_2\partial y_2}\right)\right)=-\frac{\beta\sqrt{\alpha}}{2(1+\alpha)}+\frac{i\beta\alpha}{2(1+\alpha)},$$

$$G_{21}=\frac{1}{8}\left(\frac{\partial^3P_1}{\partial x_2^3}+\frac{\partial^3P_1}{\partial x_2\partial^2y_2}+\frac{\partial^3Q_1}{\partial^2x_2\partial y_2}+\frac{\partial^3Q_1}{\partial y_2^3}+i\left(\frac{\partial^3Q_1}{\partial x_2^3}+\frac{\partial^3Q_1}{\partial x_2\partial^2y_2}-\frac{\partial^3P_1}{\partial x_2^2\partial y_2}-\frac{\partial^3P_1}{\partial y_2^3}\right)\right)=0.$$

Then, we solve

$$h_{11} = \frac{1}{4}\left(\frac{\partial^2 R_1}{\partial x_2^2} + \frac{\partial^2 R_1}{\partial y_2^2}\right) = -\frac{\beta\alpha}{2(1+\alpha)},$$

$$h_{20} = \frac{1}{4}\left(\frac{\partial^2 R_1}{\partial x_2^2} - \frac{\partial^2 R_1}{\partial y_2^2} - 2i\frac{\partial^2 R_1}{\partial x_2 \partial y_2}\right) = -\frac{\beta\alpha}{2(1+\alpha)}.$$

By solving the following equations

$$\lambda_3 \phi_{11} = -h_{11},$$

$$(\lambda_3 - 2i\omega)\phi_{20} = -h_{20},$$

we obtain

$$\phi_{11} = -\frac{\beta\alpha}{2(1+\alpha)},$$

$$\phi_{20} = -\frac{\beta\alpha}{2(1+\alpha)(1+4\alpha)} + \frac{i\beta\alpha\sqrt{\alpha}}{2(1+\alpha)(1+4\alpha)}.$$

Moreover,

$$G_{110} = \frac{1}{2}\left(\frac{\partial^2 P_1}{\partial x_2 \partial z_2} + \frac{\partial^2 Q_1}{\partial y_2 \partial z_2} + i\left(\frac{\partial^2 Q_1}{\partial x_2 \partial z_2} - \frac{\partial^2 P_1}{\partial y_2 \partial z_2}\right)\right) = \frac{\beta}{1+\alpha} - \frac{i\beta\sqrt{\alpha}}{1+\alpha},$$

$$G_{101} = \frac{1}{2}\left(\frac{\partial^2 P_1}{\partial x_2 \partial z_2} - \frac{\partial^2 Q_1}{\partial y_2 \partial z_2} + i\left(\frac{\partial^2 Q_1}{\partial x_2 \partial z_2} + \frac{\partial^2 P_1}{\partial y_2 \partial z_2}\right)\right) = \frac{\beta}{1+\alpha} - \frac{i\beta\sqrt{\alpha}}{1+\alpha},$$

$$g_{21} = G_{21} + 2G_{110}\phi_{11} + G_{101}\phi_{20} = \frac{\frac{\beta^2\alpha(-8\alpha-3)}{2} + \beta^2\alpha^2}{(1+\alpha)^2(1+4\alpha)} + i\frac{\left(-\frac{\beta^2\alpha\sqrt{\alpha}(-8\alpha-3)}{2} + \beta^2\alpha\sqrt{\alpha}\right)}{(1+\alpha)^2(1+4\alpha)}.$$

By using the above analysis, we can calculate the following quantities below

$$M_1(0) = \frac{i}{2\omega}\left(g_{20}g_{11} - 2|g_{11}|^2 - \frac{1}{3}|g_{02}|^2\right) + \frac{1}{2}g_{21} = -\frac{\beta^2\alpha}{8\alpha^2+10\alpha+2} + i\left(\frac{\beta^2\sqrt{\alpha}(2\alpha^2+\alpha-1)}{6(1+\alpha)^2(1+4\alpha)}\right),$$

$$\mu_2 = -\frac{Re(M_1(0))}{Re(\lambda'(\delta_0))} = \frac{\beta\alpha}{2+8\alpha},$$

$$\beta_2 = 2Re\, M_1(0) = -\frac{\beta^2\alpha}{4\alpha^2+5\alpha+1} < 0,$$

$$\tau_2 = -\frac{Im(M_1(0)) + \mu_2 Im(\lambda'(\delta_0))}{\omega} = \frac{\beta^2}{6+24\alpha} > 0.$$

Now, μ_2 determines the type of Hopf bifurcation and the direction of bifurcating periodic solutions; β_2 determines the stability of the bifurcating periodic solutions; τ_2 determines the increases (decreases) of the period of bifurcating periodic solutions. If $\beta > 0$ then $\mu_2 > 0$ and β_2 is always negative, so the Hopf bifurcations is supercritical and bifurcating periodic solutions exist for $\delta > 0$. But if $\beta < 0$, then $\mu_2 < 0$, so the Hopf bifurcations is subcritical and bifurcating periodic solutions exist for $\delta > 0$. Since $\tau_2 > 0$, then the period of bifurcating closed orbits increases. Then we have the following result.

Theorem 1. System (1) exhibits a Hopf bifurcation at the equilibrium point E_1, when δ pass through δ_0,with the following properties.

i. When $\mu_2 < 0$ ($\mu_2 > 0$), then the Hopf bifurcation is subcritical (supercritical) and the bifurcating periodic solution exist for $\delta < \delta_0 (\delta > \delta_0)$.
ii. When $\beta_2 < 0$ ($\beta_2 > 0$), then the bifurcating periodic solutions are orbitally stable (unstable).
iii. When $\tau_2 < 0$ ($\tau_2 > 0$), then the bifurcating periodic solutions are decreases (increases).

We now give some examples to illustrate the result in Theorem 1. To better understand the behavior of the derived periodic orbits, close to a Hopf bifurcation, we fix the values of the system parameters here and obtain numerical result. When $\alpha = 1$ and $\beta = 0.1$, and according to Proposition 2, we have $\delta_0 = 0$. It follows from results that $\mu_2 = 0.01000$, $\beta_2 = -0.00100$, $\tau_2 = 0.0003333$, by using Theorem 1, since $\mu_2 > 0$, the Hopf bifurcation is supercritical, which means that the equilibrium point $E_1$of system (1) stable when $\delta < 0$ and the equilibrium losses its stability and a Hopf bifurcation occurs when δ increases through δ_0, i.e., a family of periodic solutions bifurcate out from the equilibrium point, as shown in Figure 1.i, phase portrait for the system (1) for $\delta = 1, \alpha = 1, \beta = 0.1$. Here we observe the behavior of the Sprott L system after a Hopf bifurcation occurs $\delta < 0$. Notice that the orbits decay to the equilibrium point E_1. Phase portrait for the system (1) when $\delta = 0$, $\alpha = 1, \beta = 2$ in Figure 1.ii . At the

Hopf bifurcation point ($\delta_0 = 0$), we can see how the system (1) behaves in this instance. The trajectories remain close to the periodic solution around the attractor E_1. Phase portrait for the system (1) when $\delta = -1,\ \alpha = 1, \beta = 0.1,$ see Figure 1.iii. Before a Hopf bifurcation happens, we may see how the system (1) behaves in this instance ($\delta_0 > 0$).

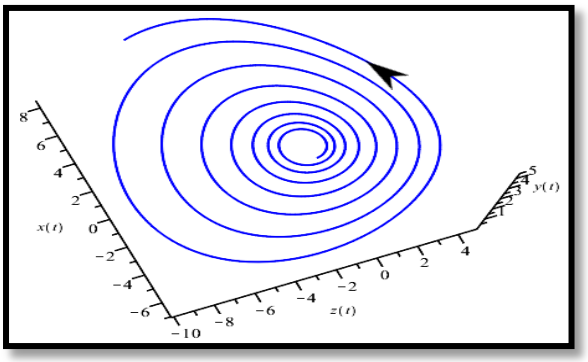

(i)

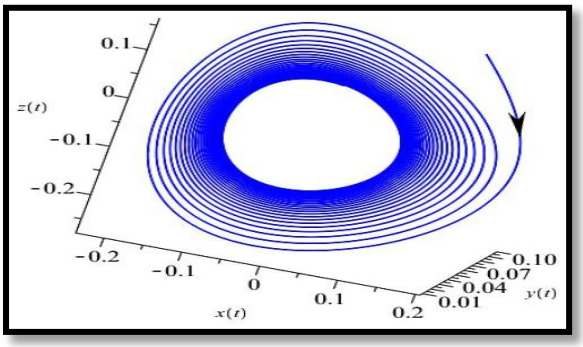

(ii)

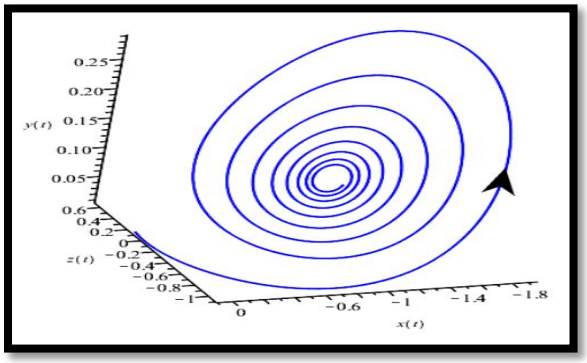

(iii)

Figure 1. Phase diagram of generalized Sprott L system (1) at the equilibrium point E_1, when (i) $\delta = 1, \alpha = 1, \beta = 0.1$ (ii) $\delta = 0, \alpha = 1, \beta = 2,$ (iii) $\delta = -1, \alpha = 1, \beta = 0.1.$

3. Dynamics Behavior Near and at Infinity

In this section, we investigate the behavior of the trajectories of system (1) near and at infinity by using the theory of Poincar´e compactification in $\mathbb{R}^3$ (Messias, 2011).

We consider the polynomial differential system

$$\dot{x} = P(x, y, z), \quad \dot{y} = Q(x, y, z), \quad \dot{z} = R(x, y, z),$$

or equivalently the associated vector field

$$\chi = P(x, y, z)\frac{\partial}{\partial x} + Q(x, y, z)\frac{\partial}{\partial y} + R(x, y, z)\frac{\partial}{\partial z}.$$

Let n be the degree of χ and we define n =max {deg (P, Q, R)}. So, the Poincar´e ball is defined as

$$\mathbb{S}^3 = \{r = (r_1, r_2, r_3, r_4) \in \mathbb{R}^4 : \| r \| = 1\},$$

be the unit sphere,

$$\mathbb{S}_+ = \{r \in \mathbb{S}^3, r_4 > 0\},\ \mathbb{S}_- = \{r \in \mathbb{S}^3, r_4 < 0\},$$

as the northern and southern hemispheres, respectively. Denote the tangent hyperplanes at the points $(\pm 1,0,0,0), (0, \pm 1,0,0), (0,0, \pm 1,0), (0,0,0, \pm 1)$ by the local charts U_i, V_i for $i = 1,2,3$ where $U_i = \{r \in \mathbb{S}^3, r_i > 0\}, V_i = \{r \in \mathbb{S}^3, r_i < 0\}.$ We only consider the local charts U_i, V_i for $i = 1,2,3$ for obtaining the dynamics at infinity.

Theorem 2. For $\beta \neq 0$, the phase portrait of system (1) on the Poincar´e compactification at infinity is as shown in Figure 7.

Proof. To prove this theorem, we will study the Poincar´e compactification of system (1) in the local charts U_i and V_i where $i = 1,2,3$. In order to understand its global behavior.

First in the local charts U_1 and V_1, we take the change of variables $(x, y, z) = (\frac{1}{w}, \frac{u}{w}, \frac{v}{w})$ and by the following computations and change of variables

$$\begin{aligned} \dot{u} &= -w^d u\, P\left(\tfrac{1}{w}, \tfrac{u}{w}, \tfrac{v}{w}\right) + w^n Q\left(\tfrac{1}{w}, \tfrac{u}{w}, \tfrac{v}{w}\right), \\ \dot{v} &= -w^d v\, P\left(\tfrac{1}{w}, \tfrac{u}{w}, \tfrac{v}{w}\right) + w^n R\left(\tfrac{1}{w}, \tfrac{u}{w}, \tfrac{v}{w}\right), \quad (8) \\ \dot{w} &= -w^{d+1} P\left(\tfrac{1}{w}, \tfrac{u}{w}, \tfrac{v}{w}\right). \end{aligned}$$

The expression of the Poincar´e compactification $p(\mathcal{X})$ of system (1) in the local chart U_1 is given by

$$\begin{aligned} \dot{u} &= -u^2 w - \alpha v u w + \beta - u w, \\ \dot{v} &= -v u w - \alpha v^2 w + \delta w^2 - w, \quad (9) \end{aligned}$$

$$\dot{w} = -uw^2 - \alpha vw^2.$$

In the points on the sphere $\mathbb{S}^2$ that corresponding to the points at infinity we have $w = 0$, and so system (9) becomes

$$\dot{u} = \beta,$$
$$\dot{v} = 0. \qquad (10)$$

Since $\beta \neq 0$, so system (10) has no equilibrium point. It follows from the Flow Box Theorem that the dynamics of the system on the local chat U_1 is equivalent to the one shown in Figure 2 whose solutions are given by parallel straight lines. We find the general directions of the vector field and the local and global trajectory structure shown in Figure 2.

Now if we study the flow in the local chart V_1, we know that it the same as the flow in the local chart U_1, because the compacted vector field $p(\mathcal{X})$ in V_1 coincides with the vector field $p(\mathcal{X})$ in U_1 multiplied by -1. Hence the phase portrait on the local chart V_1 is the same as the one shown in Figure 2, reversing the direction of the time.

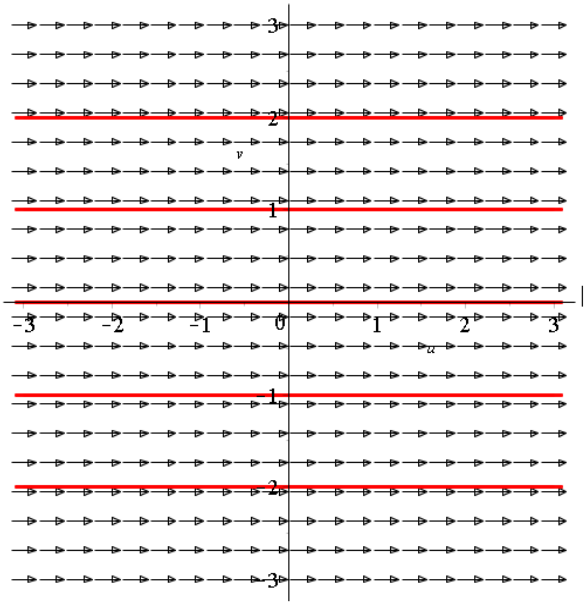

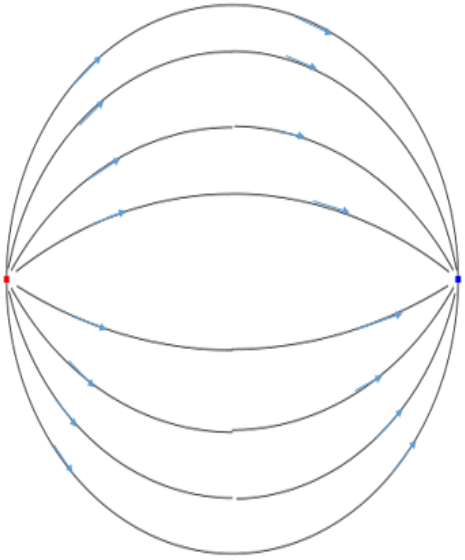

Figure 2. Dynamics of system (1) on the Poincar´e sphere at infinity in the local and the global charts U_1 for $\beta = 1$.

Second in the local charts U_2 and V_2, with the change of variables $(x, y, z) = (\frac{u}{w}, \frac{1}{w}, \frac{v}{w})$ and by the following computations and changes

$$\dot{u} = -w^d u\, Q\left(\frac{u}{w}, \frac{1}{w}, \frac{v}{w}\right) + w^n P\left(\frac{u}{w}, \frac{1}{w}, \frac{v}{w}\right),$$
$$\dot{v} = -w^d v\, Q\left(\frac{u}{w}, \frac{1}{w}, \frac{v}{w}\right) + w^n R\left(\frac{u}{w}, \frac{1}{w}, \frac{v}{w}\right), \quad (11)$$
$$\dot{w} = -w^{d+1} Q\left(\frac{u}{w}, \frac{1}{w}, \frac{v}{w}\right).$$

The expression of the Poincar´e compactification $p(\mathcal{X})$ of system (1) in the local chart U_2 is given by

$$\dot{u} = -\beta u^3 + \alpha vw + w + uw,$$
$$\dot{v} = -\beta vu^2 + vw + \delta w^2 - uw, \quad (12)$$
$$\dot{w} = -\beta u^2 w + w^2.$$

For $w = 0$ (which corresponds to the points on the sphere $\mathbb{S}^2$ at infinity) system (12) becomes

$$\dot{u} = -\beta u^3,$$
$$\dot{v} = -\beta vu^2. \qquad (13)$$

After eliminating the common factor βu^2 of system (13) (by rescaling of the time) we obtain

$$\dot{u} = -u,$$
$$\dot{v} = -v. \qquad (14)$$

System (14) has a unique equilibrium point (0,0), and has the two eigenvalues of the Jacobian matrix at the equilibrium point origin of system (11) are equal -1, hence the origin is stable node of system (14). Hence, due to the common factor u^2, the local behavior of the solutions near to the origin of system (13) is constituted by parabolic

repelling sector in $\{u > 0\}$ and parabolic attractor sector in $\{u < 0\}$. The local and global trajectories are shown in Figure 3.

Also, if we study the flow in the local chart V_2, we know that it the same as the flow in the local chart U_2, because the compacted vector field $p(\mathcal{X})$ in V_2 coincides with the vector field $p(\mathcal{X})$ in U_2 multiplied by -1. Hence the phase portrait on the local chart V_2 is the same as the one shown in Figure 3, reversing the direction of the time.

In briefly the equilibria at infinity at the positive and (respectively negative) endpoints of the $y-$axis are stable and (respectively unstable) node. See Figure 3.

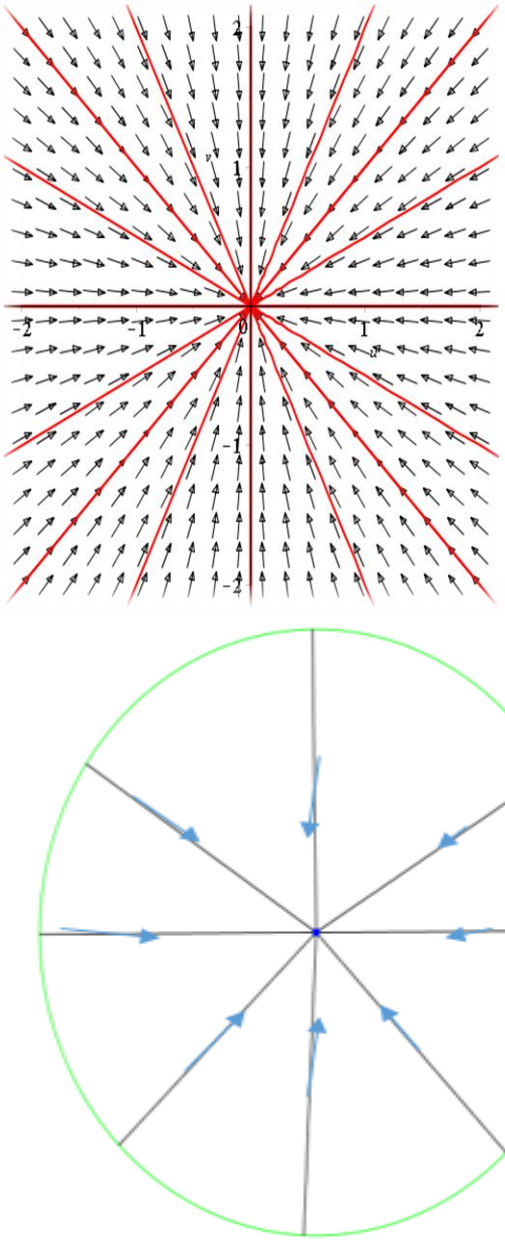

Figure 3. Dynamics of system (1) on the Poincar´e sphere at infinity in the local and the global charts U_2.

Finally, in the local charts U_3 and V_3, we consider infinity at z axis. Let $(x, y, z) = (\frac{u}{w}, \frac{v}{w}, \frac{1}{w})$, so by the following computations and changes

$$\begin{aligned} \dot{u} &= -w^d u\, R\left(\tfrac{u}{w}, \tfrac{v}{w}, \tfrac{1}{w}\right) + w^n P\left(\tfrac{u}{w}, \tfrac{v}{w}, \tfrac{1}{w}\right), \\ \dot{v} &= -w^d v\, R\left(\tfrac{u}{w}, \tfrac{v}{w}, \tfrac{1}{w}\right) + w^n Q\left(\tfrac{u}{w}, \tfrac{v}{w}, \tfrac{1}{w}\right), \\ \dot{w} &= -w^{d+1} R\left(\tfrac{u}{w}, \tfrac{v}{w}, \tfrac{1}{w}\right). \end{aligned} \quad (15)$$

The expression of the Poincar´e compactification $p(\mathcal{X})$ of system (1) in the local chart U_3 is given by

$$\begin{aligned} \dot{u} &= -\delta u w^2 + u^2 w + v w + \alpha w, \\ \dot{v} &= -\delta v w^2 + v u w + \beta u^2 - v w, \\ \dot{w} &= -\delta w^3 + u w^2. \end{aligned} \quad (16)$$

Also, in the points of the sphere $\mathbb{S}^2$ that corresponds to the points at infinity we have $w = 0$, and so system (16) becomes

$$\begin{aligned} \dot{u} &= 0, \\ \dot{v} &= \beta u^2. \end{aligned} \quad (17)$$

System (17) has a line of non-hyperbolic equilibria given by the $(0, v)$ and the Jacobian matrix of the system (17) at these equilibria has two null eigenvalues. System (17) is integrable, because if $u \neq 0$ it has the first integral $u = c$, where c is constant.

By using the first integral and we know that system (17) has the $v-$axis as a line of equilibria and the local and global trajectories are shown in figure 4.

Now, if we investigate the flow in the local chart V_3, we know that it the same as the flow in the local chart U_3 reversing the time, because the compactified vector field $p(\mathcal{X})$ in V_3 coincides with the vector field $p(\mathcal{X})$ in U_3 multiplied by -1. Hence, the phase portrait on the chart V_3 is the same as shown in Figure 4, reversing the time direction.

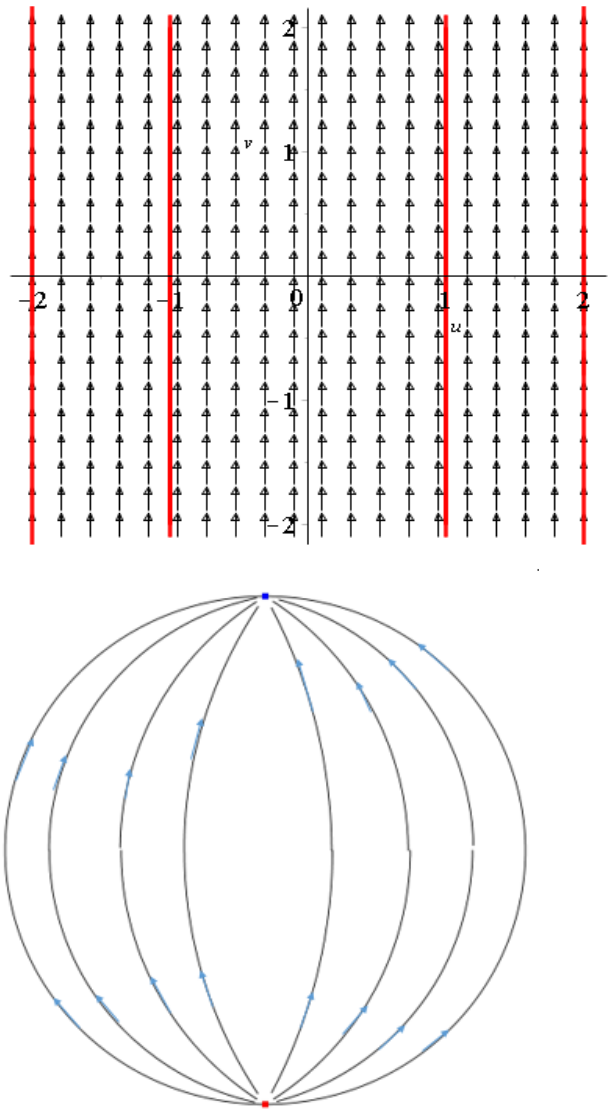

Figure 4. Dynamics of system (1) on the Poincar´e sphere at infinity in the local and the global charts U_3 for $\beta = 1$.

From the above analysis in all charts and taking into account its orientation shown in Figure 6 in all local charts at the positive endpoints of the x, y, z axes, we can get the structure of system (1) on the sphere at infinity shown in Figure 6. The system has two nodes on the sphere and there are no periodic orbits. We observe that the description of the complete phase portrait of system (1) on the sphere at infinity was possible because of the invariance of these sets under the flow of the compactified system. This proves Theorem 2.

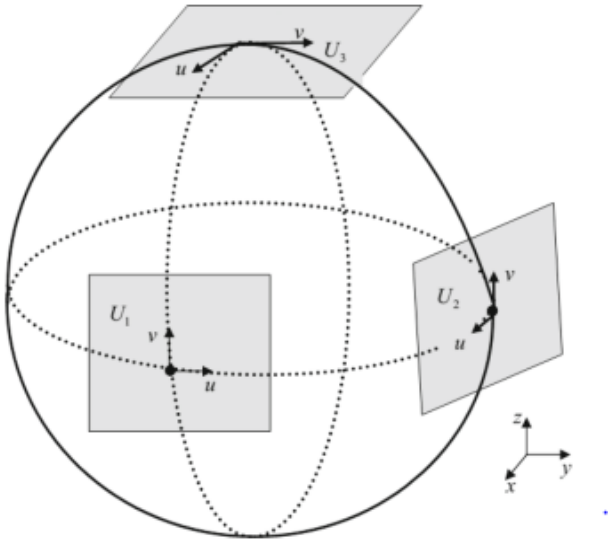

Figure 5. Orientation of the local charts U_i, i = 1, 2, 3 in the positive endpoints of coordinate axis x, y, z.

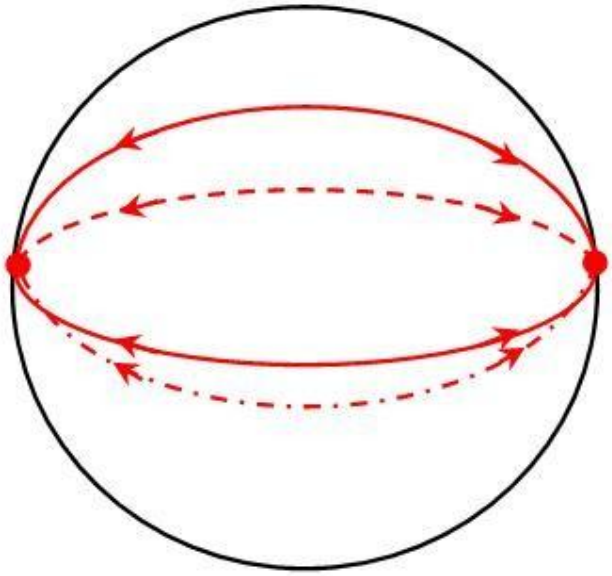

Figure 6. Global phase portrait of system (1) on the Poincar´e sphere at infinity

It is significant to note that the global dynamics at infinity do not depend on the parameters in system (1). Figure 6 also shows a pair of distinct equilibriums and two closed curves filled with equilibria.

4. Conclusion

New insights into the generalized Sprott *L* differential system are presented. Firstly, the equilibrium points and their linear stabilities of system are determined. Also, the Hopf bifurcation analysis of system (1) has been studied by applying normal form theory. We analyzed the direction of Hopf bifurcation and the stability of

bifurcating periodic solutions in detail. Finally, the Poincare compactification approach has been used to study the global dynamics at infinity.

References

Amen, A.I. & Salih, R. H., 2008. Limit cycles of Lorenz system with Hopf bifurcation. Al-Rafiden Journal of Computer Sciences and Mathematics volume 5, pp.81-99.

Cima, A. & Llibre, J., 1990. Bounded polynomial vector fields. Transactions of the American Mathematical Society, 318(2), pp.557-579.

Guckenheimer, J. & Holmes, P., 2013. . Nonlinear oscillations, dynamical systems, and bifurcations of vector fields (Vol. 42). Springer Science & Business Media.

Hassard, B. & Wan, Y. H., 1978. Bifurcation formulae derived from center manifold theory. Journal of Mathematical Analysis and Applications, Volume 63(1), pp.297- 312.

Jiang, B., Han, X. 2010. Hopf bifurcation analysis in the T system. Nonlinear Analysis: Real World Applications, Volume 11(1), 522-527.

Messias, M., 2011. Dynamics at infinity of a cubic Chua's system. International Journal of Bifurcation and Chaos, 21(01), pp.333-340.

Mirkhan, J. M. & Amen, A.I., 2022. Bifurcation analysis for Shil'nikov Chaos Electro-dissolution of copper. Zanco Journal of Pure and Applied Sciences, Volume 34(4), 83-91.

Moiola, J.L. & Chen, G., 1996. Hopf bifurcation analysis: a frequency domain approach (Vol. 15). World Scientific.

Sprott, J. C., 1994. Some simple chaotic flows. Physical review E, Volume 50(2),p.R647.

Vaidyanathan, S., 2012. Global chaos synchronization of Sprott-L and Sprott-M systems by active control. International Journal of Control Theory and Computer Modelling (IJCTCM) Vol, 2.